PROCEEDINGS, Thirty-Sixth Workshop on Geothermal Reservoir Engineering
Stanford University, Stanford, California, January 31 - February 2, 2011
SGP-TR-191

RESERVOIR ASSESSMENT OF THE OLFUS-BAKKI LOW-TEMPERATURE GEOTHERMAL AREA, SW ICELAND

Javier Gonzalez-Garcia[1], Gudni Axelsson[2], Gunnar Gunnarsson[3], and Einar Gunnlaugsson[3]

1) REYST – Bæjarháls 1 – 110 Reykjavík – Iceland
2) Iceland GeoSurvey – Grensásvegi 9 – 108 Reykjavík – Iceland
3) Reykjavík Energy – Bæjarháls 1 – 110 Reykjavík – Iceland
e-mail: jag13@hi.is

Keywords: Olfus, Bakki, low temperature, well-logging, geothermal cartography, volumetric assessment, lumped parameter modeling, conceptual model, Hveragerdi, Thorlakshofn.

ABSTRACT

The Olfus-Bakki geothermal area (OBGA) in SW Iceland is located in the S and SE margins of the high-enthalpy systems of Hveragerdi and Hengill, respectively. This geothermal area contains a productive region, denominated the Bakki field, which produces fluid at temperatures in the range of 100-130 °C. Since 1979, the geothermal resource has supplied thermal energy to the town of Thorlakshofn, mainly for space heating and aquaculture. The central objective of this study is to provide a reservoir assessment supported by the integration of the available information. The methodology included 1) the interpretation of well logging data for pressure and temperature, 2) the interpretation of geochemical data, 3) the mapping of baric, thermal and geochemical anomalies, 4) the preparation of a volumetric assessment of the reservoir and 5) the preparation of a lumped parameter model for the Bakki field. The combination of these methods allows an improved understanding of the natural state of the reservoir as well as its response to production under different scenarios. Data from nearly 24 wells was analyzed. Given the availability of data, the scope of the present assessment is constrained to the uppermost 1000 m of the reservoir. Analysis of the patterns of pressure and formation temperature allowed the identification of a convective system migrating southwards, very likely associated to the neighboring high-enthalpy geothermal system at Hveragerdi. Chemical analyses permitted characterizing the fluids from the entire region into distinctive units. This characterization provided valuable clues to discern fluid provenance, as well as to identify possible recharge zones. Results from the volumetric assessment, based on a Monte Carlo simulation, indicated a mean reservoir capacity between 210-730 MW_{th} for lifetimes between 30-100 years, with a 90% confidence interval of 98-1200 MW_{th}. Lumped parameter modeling indicates that Olfus-Bakki is an open system with unconfined aquifers. Current utilization is considered to be sustainable for the next 300 years given that production maintains the same rate of growth observed over the past 20 years.

INTRODUCTION

The OBGA comprises the regions of low temperature geothermal activity S of Hveragerdi. This study focuses on the Bakki field, currently exploited by three production wells (viz. HJ-01, BA-01, and EB-01). Figure 1 presents a spatial reference for the features and wells mentioned in this paper.

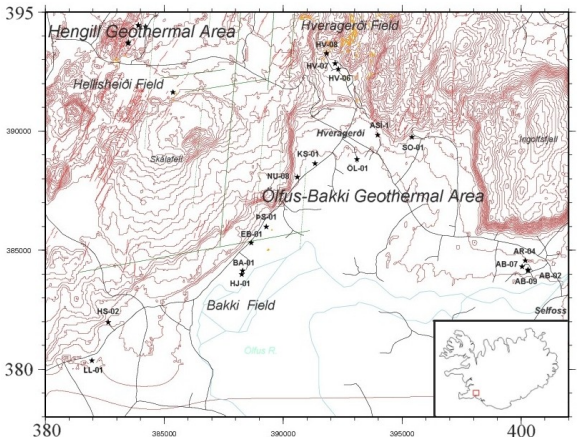

Figure 1: Location of the OBGA and surroundings. Coordinates: ISNET (km).

The Bakki field has produced thermal fluid for the open district heating system of Thorlakshofn, in the SW coast of Iceland. Currently, there is no effluent reinjection in the area. Locally, part of the resource is used for aquaculture through shallow wells producing lower temperature fluid. The scale of this activity is

much lower than space heating. Therefore, the effect of the smaller, shallower wells is neglected during the modeling process.

This report contains an abridged version of the MSc thesis project work conducted by the author at REYST, and supervised by the authors at Iceland GeoSurvey and Reykjavik Energy, during the Fall-2010 semester (Gonzalez-Garcia, 2011).

WELL-LOG INTERPRETATION

The OBGA contains approximately 90 wells. Well-logging data of pressure and temperature conditions was available for 24 wells. This data was used to estimate formation temperature and feed zones at each location. Figure 2 shows the interpretation of the records of well EB-01 in the Bakki field as an example of the procedure employed.

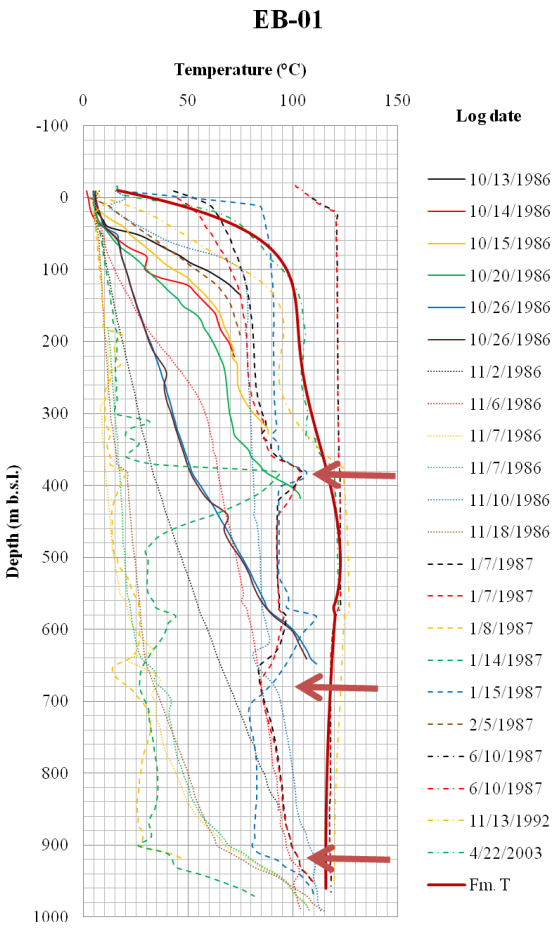

Figure 2: Formation temperature (thick solid red line) and location of major feed zones (arrows) as interpreted from well-logging data. Well EB-01, Bakki field.

Formation temperature was inferred based on patterns of thermal recovery, following the methodology proposed by Stefánsson and Steingrímsson (1990).

PRESSURE AND TEMPERATURE MAPPING

The calculated formation temperature values were sampled at 100 m intervals down to 1000 m.b.s.l. at each well location. This data was converted to control points in the form (x, y, z) required to generate a surface, where the x,y coordinates represent wellhead location and the z coordinate represents formation temperature. Interpolated surfaces were generated representing formation temperature distribution at given depths. A similar procedure was carried using pressure well-logs.

Additional control points outside the study area were defined as boundary conditions to improve the results of the surface interpolation. The first type of boundary condition was a series of control points with values from the neighboring Hengill area. The second type was a line with points with constant gradient along a NEE-SWW-trending line located approximately 5 km south of the Bakki field. The geothermal gradient along this line was defined as 85 °C/km, while the pressure gradient was defined as the weight of a column of cold water at a given depth. The information extracted from the well-logging interpretation process was later used to produce a temperature and pressure model for the study area. This model is presented as a tomography of the reservoir (Figure 3).

The distribution of pressure and temperature shows higher values to the north, around the Hveragerdi field. These values decrease more or less homogeneously to the south, close to the Olfus River. This distribution implies that the high-temperature Hveragerdi area acts as a heat source for the OBGA. Additionally, the presence of an area of low pressure around the Bakki field (especially below 600 m.b.s.l.) suggests that fluids from the surrounding regions might converge at this point.

GEOCHEMICAL DATA INTERPRETATION

Records containing geochemical data were available from 19 locations. Several constituents are present in the analyses, being categorized in a) rock-forming constituents, b) incompatible elements, c) heavy isotopes, d) dissolved gases. Different methods of interpretation were adopted. These include a) concentration mapping, b) Cl/B analysis, c) δD and $\delta^{18}O$ analysis, d) Na-K-Mg and Cl-HCO_3-SO_4 geoindicator analysis.

Maps indicating the concentrations of selected constituents are presented in Figure 4. These maps

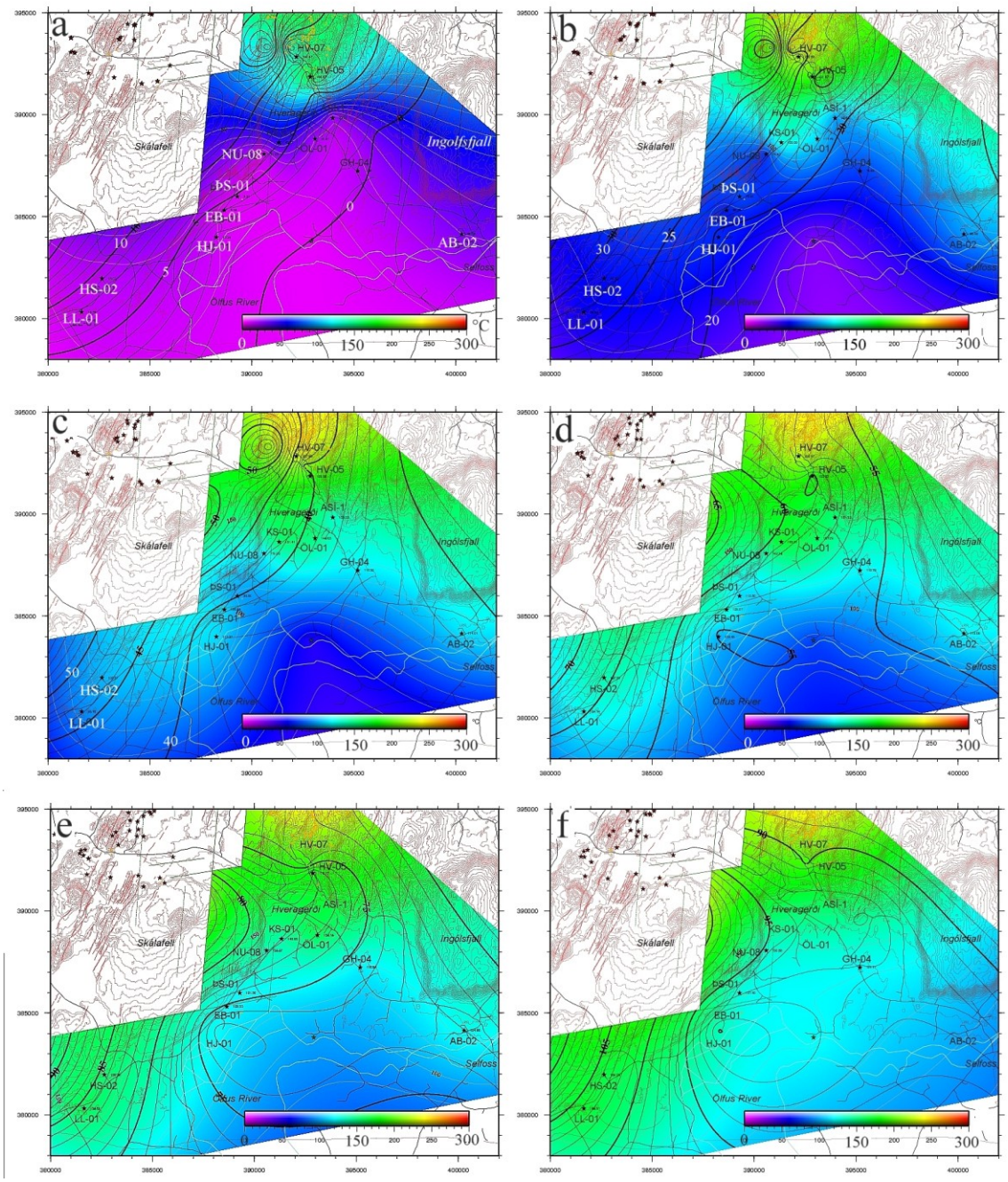

Figure 3: *Temperature and pressure model for the OBGA. Model presented as a tomography at given depths. a) 0 m.b.s.l., b) 200 m.b.s.l., c) 400 m.b.s.l., d) 600 m.b.s.l., e) 800 m.b.s.l., f) 1000 m.b.s.l..*

were prepared using a similar method as the one referred above. The value of the z-coordinate was given by the average of the concentration values available at each location. The boundary conditions were determined by some control points in the Hengill area and along the same NEE-SWW-trending line defined above. The formation transected by this line was assumed to be saturated with marine water.

Some regional trends are observed in these maps. The distribution of silica (Fig. 4a) shows relatively high concentrations towards the highland zones, where higher temperatures are found. The chlorine distribution shows the lowest values in the Ingolfsfjall region to the NE of the study area. There are also minor anomalies around well ÞS-01 and around well HS-02 (Hlidardalskoli). Chlorine

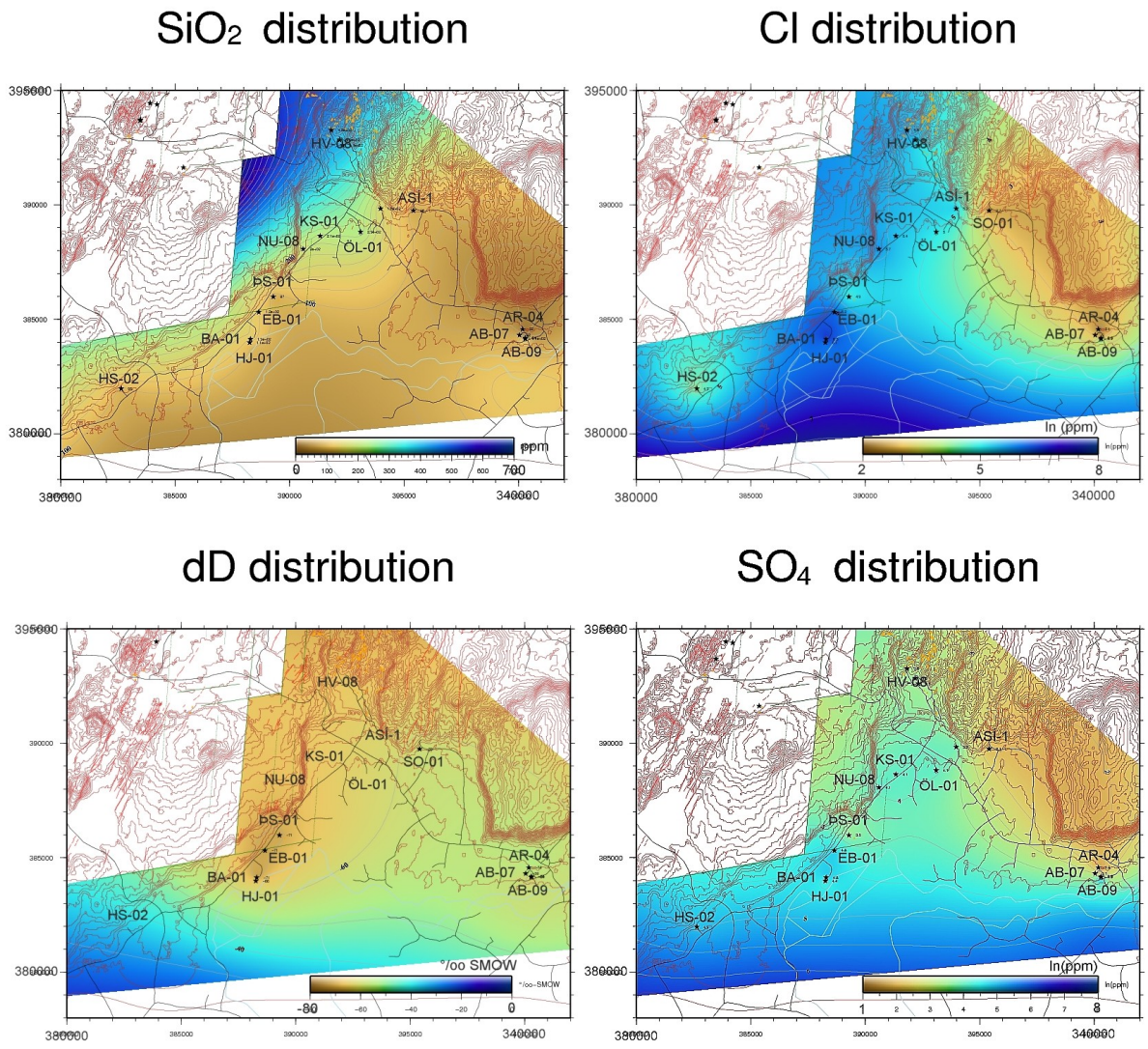

Figure 4: Geographical distribution of groundwater concentrations of a) silica, b) chlorine, c) deuterium deviation from SMOW, d) sulfate. ISNET coordinate system

concentration is related to both fluid salinity and water-rock interaction.

The deuterium distribution shows a regional trend with relative depletion increasing further inland. The distribution of sulfate shows low concentrations around the Ingolfsfjall zone and to the N of well ÞS-01.

Another method was the analysis of Cl/B molal ratio. This method has been proven and validated in Iceland to aid in the identification of the provenance of groundwater in geothermal systems (Arnórsson and Andrésdóttir, 1995). The value of this ratio in marine water is 1300, and it approximately 30 in basaltic rock. The variations in the value of this ratio were mapped and are presented in Figure 5.

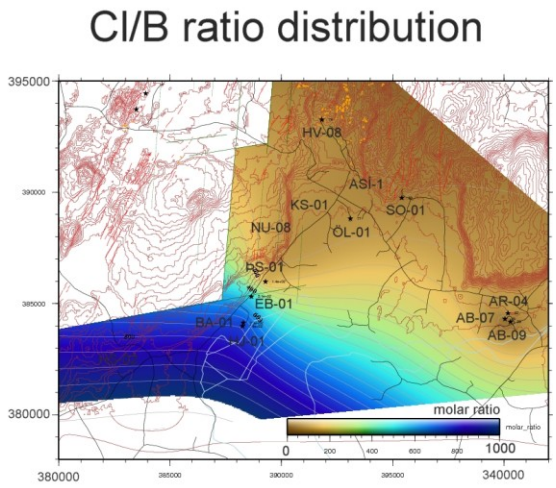

Figure 5: Geographical distribution of the Cl/B molal ratio.

Figure 5 also shows the extent of marine influence in groundwater from the OBGA. As it could be expected, the value of Cl/B decreases further inland. The relation between deuterium and oxygen-18 can be seen in Figure 6.

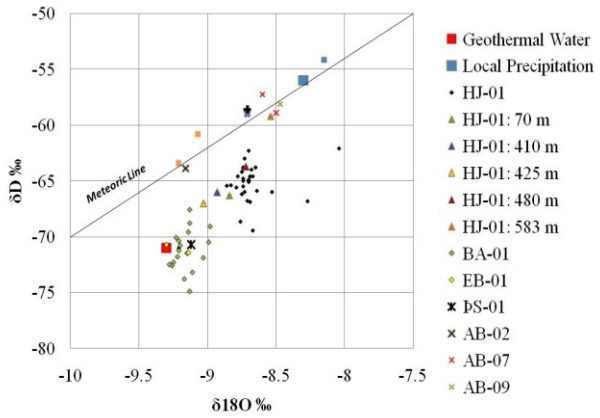

Figure 6: Relationship between δD and $\delta^{18}O$ for the samples from the OBGA.

Figure 6 indicates that most samples in the OBGA present the oxygen shift characteristic of water-rock interaction. An exception to this trend comes from the samples in the Ingolfsfjall region, which correlate with the meteoric line.

The fluids in the area were characterized using Na-K-Mg and Cl-HCO_3-SO_4 geoindicators (Giggenbach, 1988; Giggenbach, 1991; Arnosson et al, 1998). The samples across the study area were normalized and plotted in ternary diagrams (Figure 7). Five distinct groups were identified, namely Bakki field (black), Nupafjall zone (green), Hlidardalskoli (brown), Hveragerdi (orange) and Ingolfsfjall zone (blue).

a

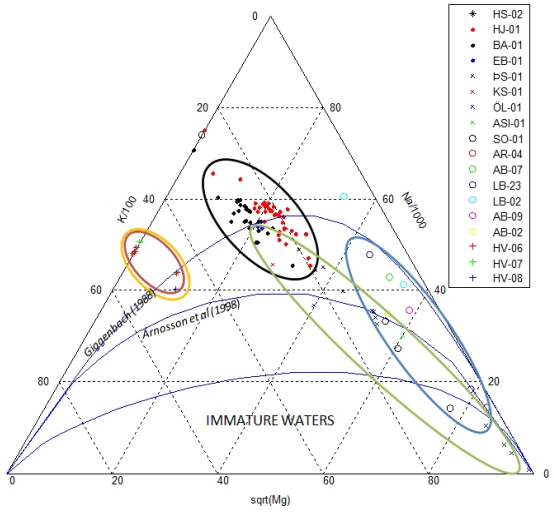

b

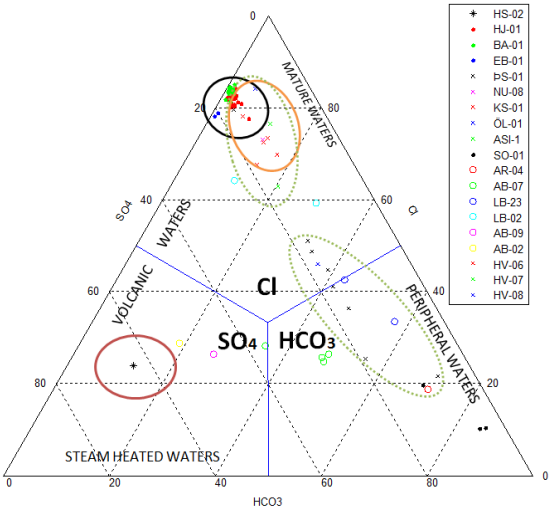

Figure 7: Characterization of fluids by geoindicators. a) Na-K-Mg; b) Cl-HCO_3-SO_4. Chemically-related samples are grouped. (Black: Bakki field. Green: Nupafjall region. Orange: Hveragerdi. Brown: Hlidardalskoli. Blue: Ingolfsfjall.

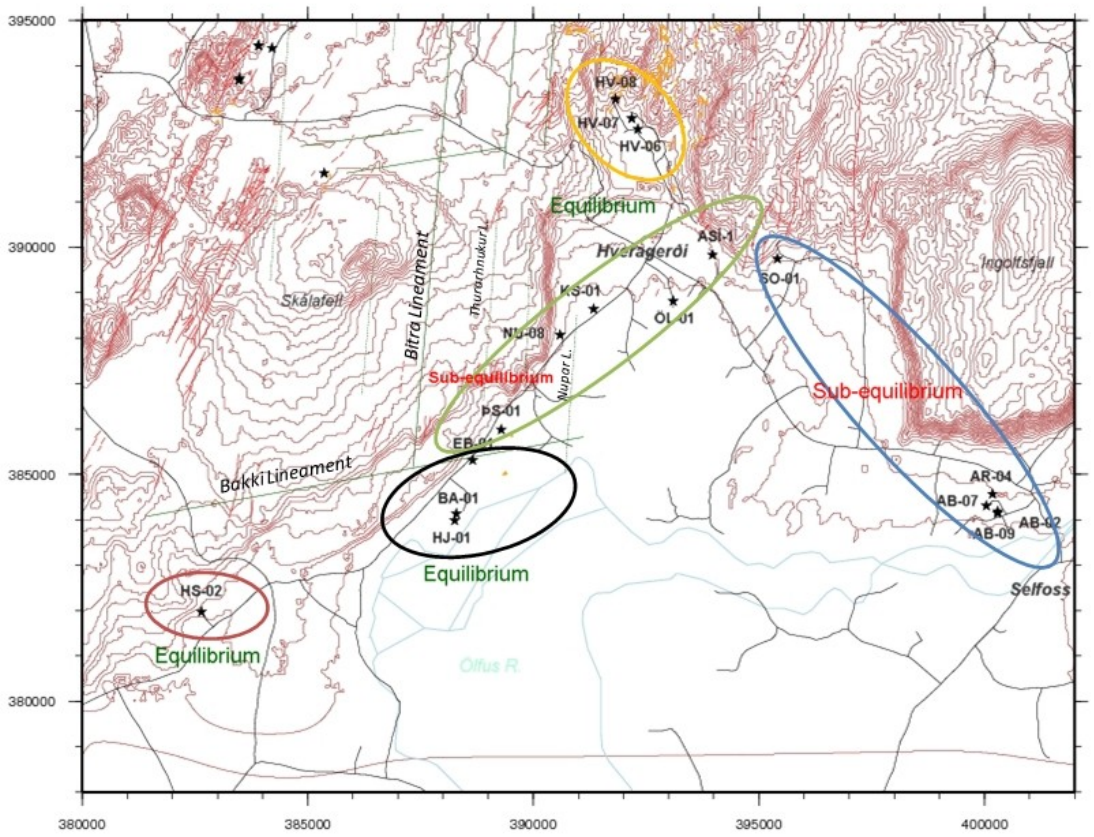

Figure 8: Geographic distribution of the geochemical zones identified through Na-K-Mg and Cl-HCO_3-SO_4 geoindicators. Color reference is described in Figure 7.

The Na-K-Mg analysis indicates that the waters from Bakki, Hlidardalskoli and Hveragerdi have attained equilibrium with the secondary minerals in the formation. The waters from the Nupafjall zone are close to equilibrium, except for those from well ÞS-01. Meanwhile, the waters from the Ingolfsfjall zone have not reached that state. Similarly, the Cl-HCO_3-SO_4 classification shows that the equilibrated samples are chlorinated waters of volcanic origin (except for Hlidardalskoli, which was classified as sulfate water). Samples from well ÞS-01 and from the Ingolfsfjall zone are classified as peripheral waters.

Figure 8 shows the spatial distribution of these results. It can be observed that the Bakki lineament separates the wells EB-01 and ÞS-01. Given the compositional differences of waters from both wells, it can be proposed that this lineament is the N boundary of the Bakki field.

From the evidence at hand, it is deduced that volcanic, chlorinated waters from Hveragerdi migrate to the south following the hydraulic gradient. Groundwater flow is restricted by deep faults and tectonic lineaments. Meteoric water might enter the system through surface faults and fractures, and might mix with the volcanic water in the Ingolfsfjall area. A similar pattern is observed around well ÞS-01. Waters of volcanic, marine and volcanic-meteoric origin converge in the Bakki field due to the effect of the hydraulic gradient. The geochemical differences between the waters from wells EB-01 and ÞS-01 suggest the absence of mixing. Additionally, the presence of a buried tectonic lineament separating these wells (Bakki lineament) might be indicative of such structure restricting the southbound component of groundwater flow.

VOLUMETRIC ASSESSMENT

In order to estimate the heat capacity of the Bakki field it is necessary to define its boundaries. As previously mentioned, the Bakki lineament bounds the field to the N. The other boundaries, however, are not distinctively defined. To the W geochemical characterization shows differences between the fluids at Bakki and Hlidardalskoli, suggesting the presence of a boundary somewhere between these regions. The influence of marine water increases with proximity to

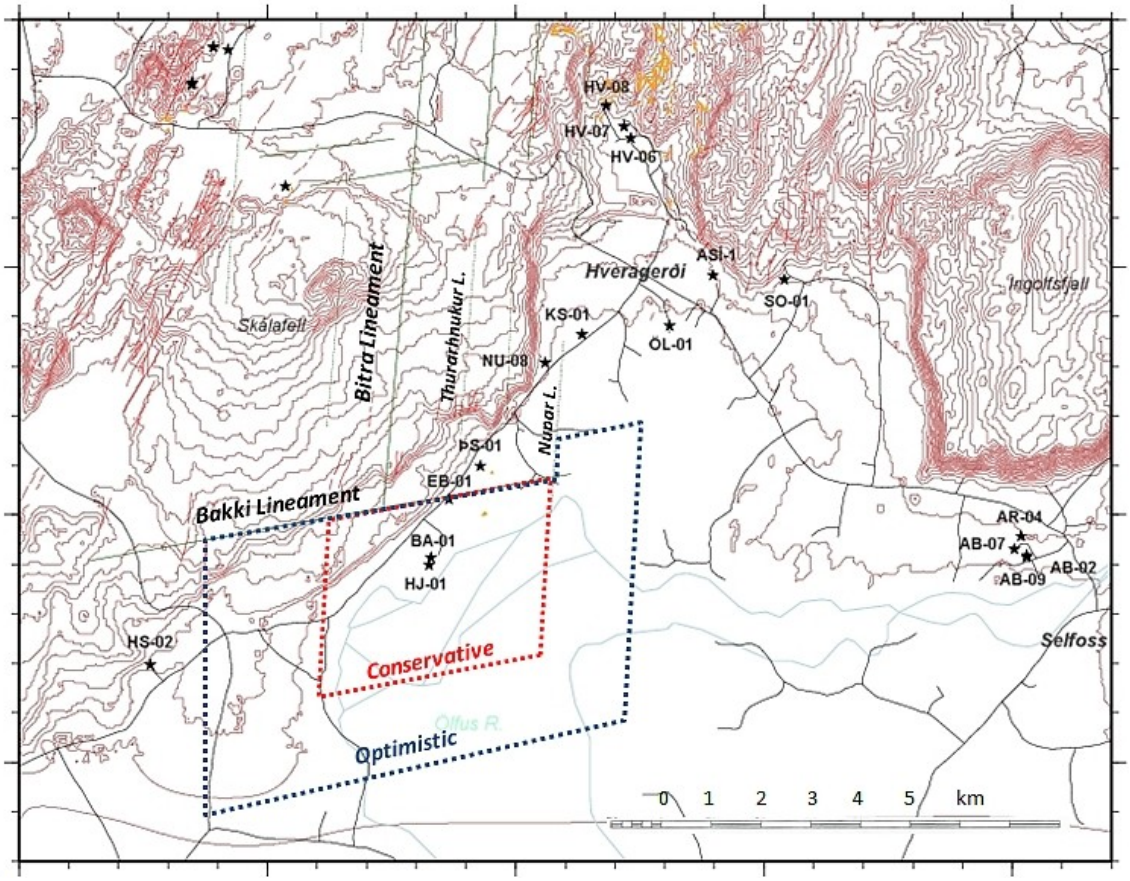

Figure 9: Proposed boundaries of the Bakki geothermal field. The field surface area measures 16.4 km^2 for the conservative estimate, and 45.5 km^2 for the optimistic estimate.

the coast, suggesting a transitional southern boundary. To the E there is a marked difference between the waters from Bakki and the Ingolfsfjall zone, besides a small pressure gradient between these regions.

Because the nature of some of these boundaries is uncertain, it is proposed that the Bakki field is delimited by both an optimistic and a conservative boundary. The actual limits of the field are expected to lie somewhere within this region (Figure 9).

The next step is calculating the amount of recoverable heat contained in the reservoir. Recoverable heat is given by the product of total heat content in the reservoir, recovery factor (i.e. percentage of accessible energy that is technically recovered) and surface accessibility (i.e. proportion of the reservoir that can be accessed by drilling from the surface).

(1) $$E_{recoverable} = E_{res} A R$$

Since the area is relatively flat and numerous roads pass through, surface accessibility is expected to lie between 90-100%. A recovery factor in the range of 5-20 % is assumed. The total heat content in the reservoir is the combined heat of both the formation and the fluid.

The heat content in the formation and in the fluid is calculated by the expressions:

(2) $$E_{reservoir} = E_{rock} + E_{fluid}$$

(3) $$E_{rock} = V(1-\varphi)\rho_{rock}\beta_{rock}(T_{reservoir} - T_{reference})$$

(4) $$E_{fluid} = V\varphi\rho_{fluid}\beta_{fluid}(T_{reservoir} - T_{reference})$$

Where V is the volume, φ represents porosity, ρ represents density, β represents heat capacity, and T represents temperature. The reference temperature is defined as the annual average of the surface temperature in the town of Hveragerdi (i.e. 4.75 °C).

The reservoir temperature is evaluated from the temperature model presented above.

The principal use of the geothermal resource is space heating. The portion of the reservoir with temperatures greater than 80 °C is considered suitable for utilization. The areas with temperatures greater than 80 °C are measured in the temperature model, presented as a series of isothermal contours at given depths. This action produces a sequence of known areas outlining a volume that can be estimated numerically.

Figure 10 shows a projection of such volume. The same method is applied for those portions of the reservoir with temperatures greater than 100, 120 and 150 °C, respectively. This is done with the objective of reducing the uncertainty of the volume parameter in equations (3) and (4).

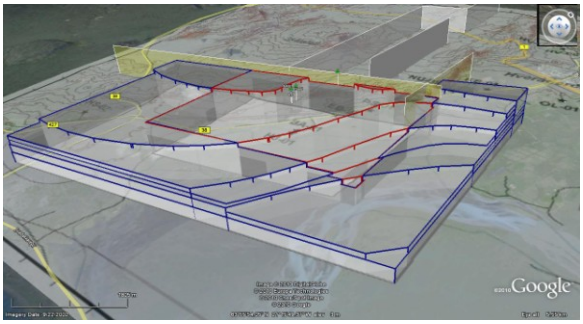

Figure 10: Projected volume of the reservoir (as defined in Fig. 9) with temperatures greater than 80 °C. The red outline represents the conservative boundary. The blue outline represents the optimistic boundary. Added content to image from Google™.

The volumetric discretization of the reservoir allows the implementation of the equations proposed by Halldórsdóttir et al (2010):

$$E_{reservoir} = \sum_{i}^{N} C_i(\varphi_i, T_i, P_i)[T_i - T_{ref}]\Delta V_i \quad (5)$$

$$C(\varphi_i, T_i, P_i) = \beta_{fluid}(T_i, P_i)\rho_{fluid}(T_i, P_i)\varphi_i + \beta_r(T_i, P_i)\rho_r(T_i, P_i)(1-\varphi_i) \quad (6)$$

Where N is the number of volume subdivisions in the reservoir, and C is the heat capacity per volume of reservoir.

A Monte Carlo simulation was used to solve equations (1), (5) and (6). The thermal power capacity of the reservoir is obtained by dividing $E_{recoverable}$ by the amount of seconds in a given lifetime. Table 1 presents the parameters employed in the simulation. Each parameter was assigned a distribution that was deemed suitable.

Table 1: Parameters used in the Monte Carlo simulation estimating thermal power capacity of the reservoir.

Parameter	Min.	Most Likely / Mean	Max.	Distribution
φ	0.05	0.10	0.15	Triangular
T_1 (°C)	80		100	Uniform
T_2 (°C)	100		120	Uniform
T_3 (°C)	120		150	Uniform
V_1 (km^3)	3.13	5.88	8.63	Normal
V_2 (km^3)	5.35	8.53	11.71	Normal
V_3 (km^3)	3.26	6.10	8.94	Normal
T_{ref} (°C)		4.75		Constant
ρ_{rock} (kg/m^3)		2800		Constant
β_{rock} (J/kg°C)		880		Constant
A	0.9	0.95	1.0	Triangular
R	0.05	0.13	0.20	Triangular
η		1		Constant

The indexed volume values represent those portions of the reservoir with temperatures between the maximum and minimum indexed temperatures. The maximum and minimum volume was the value measured for the optimistic and conservative projections, respectively (Figure 10). The utilization efficiency, η, is assumed as 1.

A population of 10,000 sets of parameters was generated using random values arranged according to the distributions indicated in Table 1. Figures 11a-11c show the probability distribution of the thermal power capacity calculated for lifetimes of 30, 50 and 100 years, respectively.

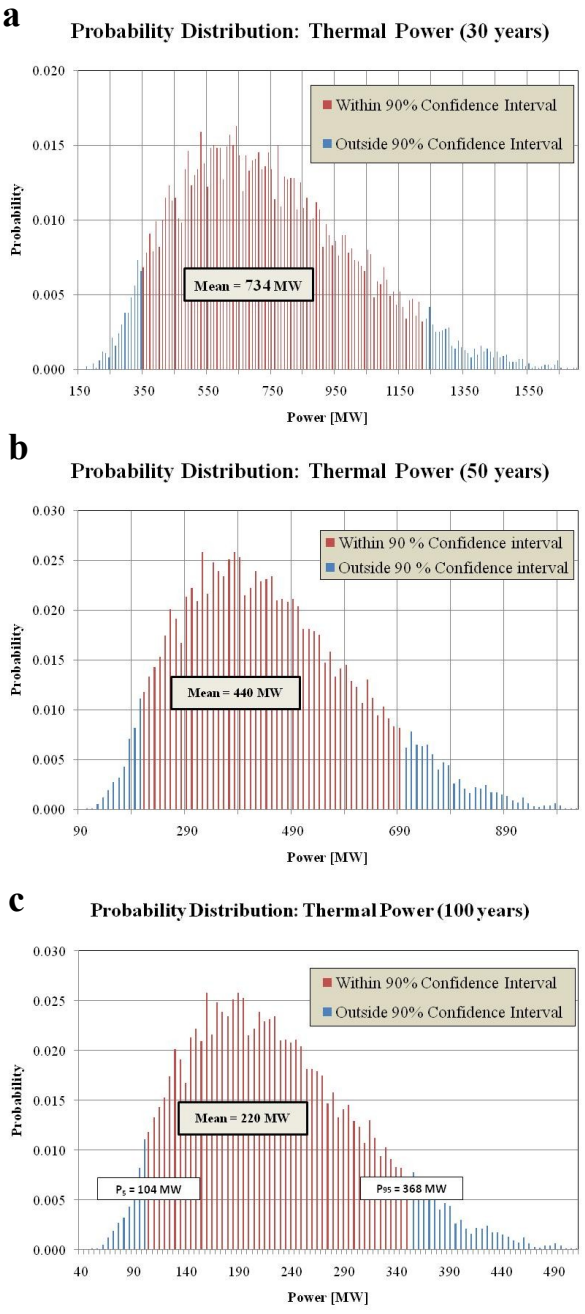

Figure 11: Probability distribution of the maximum capacity of the reservoir within lifetimes of a) 30 years, b) 50 years, c) 100 years.

The calculated reservoir thermal capacity is given as a range defined by the 90% confidence interval at each lifetime. Table 2 summarizes the results of these calculations.

Table 2: Parameters used in the Monte Carlo simulation estimating thermal power capacity of the reservoir.

	Thermal Power [MW]		
	30 years	*50 years*	*100 years*
Mean	734.24	440.55	209.63
Percentile 5	**346.05**	**207.63**	**98.26**
(As $\dot{m}$ in kg/s)	*1090*	*656*	*310*
Percentile 95	**1226.90**	**736.14**	**351.55**
(As $\dot{m}$ in kg/s)	*3880*	*2330*	*1110*
Median	702.78	421.67	200.49
St. dev.	270.98	162.59	77.95

As a point of reference, these results are compared with the average extracted thermal power over the last decade. The Bakki field has three major productive wells (viz. BA-01, HJ-01, EB-01). The combined average production rate ($\dot{m}$) between 1999 and 2009 was 37.25 kg/s, and the average fluid temperature was 110.3 °C. These are estimates evaluated using values from Aradóttir (2010a, 2010b). Equation (7) indicates that the thermal power ($\dot{Q}$) extracted from 1999 to 2009 was 16.5 MW_{th}.

(7) $$\dot{Q} = \dot{m}\beta_{fluid}(T_{fluid} - T_{reference})$$

Equation (7) can be re-arranged to express reservoir capacity in terms of production rate of fluid at 110.3 °C (Table 2).

From these results, it is evident that current utilization lies well below the thermal capacity of the reservoir. However, this volumetric assessment does not take into consideration the effects of recharge and production pressure response. This situation makes necessary the implementation of a dynamic modeling method. Due to its simplicity and effectiveness, lumped parameter modeling becomes the preferred method.

LUMPED-PARAMETER MODELING

Lumped parameter modeling is an effective and relatively simple method employed in geothermal management. Its accuracy has been validated for several study cases from around the world where data quality has been satisfactory (Axelsson et al, 2005). A detailed explanation of this method can be found in Axelsson (1989) and Axelsson and Arason (1992). The production data from wells BA-01, HJ-01 and

EB-01 has been combined and used as input for the application LUMPFIT (part of the ICEBOX package). The pressure response of the system is reflected in the water level fluctuations observed in well HJ-01. Well BA-01 is artesian and water level in well EB-01 has been recorded only since 2002; therefore, the use of the record of well HJ-01 is justified.

LUMPFIT treats the simulation as an inverse problem. The program tries to automatically fit analytical response functions to the observed data. This is achieved through a nonlinear iterative least-squares technique for model parameter estimation (Axelsson, 1989; Axelsson and Arason, 1992).

Figure 12 presents the production history from the wells in the Bakki field. Production data previous to 1989 is scarce, and is shown as the annual averages of total production. The drilling dates for wells BA-01, HJ-01 and EB-01 were 1978, 1984 and 1987, respectively. Well EB-01 remained largely unused until 2004.

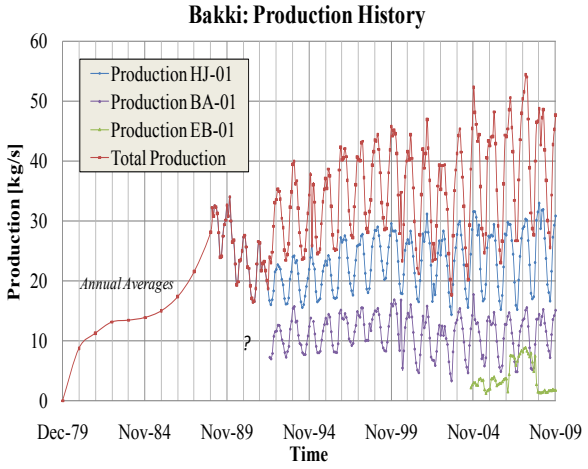

Figure 12: Production history of the Bakki field.

The modeling process started with the simplest model configuration, i.e. a 1-tank closed model. It increased in complexity up to a 2-tank model, both open and closed. It was found that more complex arrangements were not a major improvement in the model fit. Figures 13(a-b) contain the simulation results for the 2-tank closed and 2-tank open models, respectively. Lumpfit automatically evaluated the storage (κ) and mass conductance (σ) coefficients. These values are presented in Table 3.

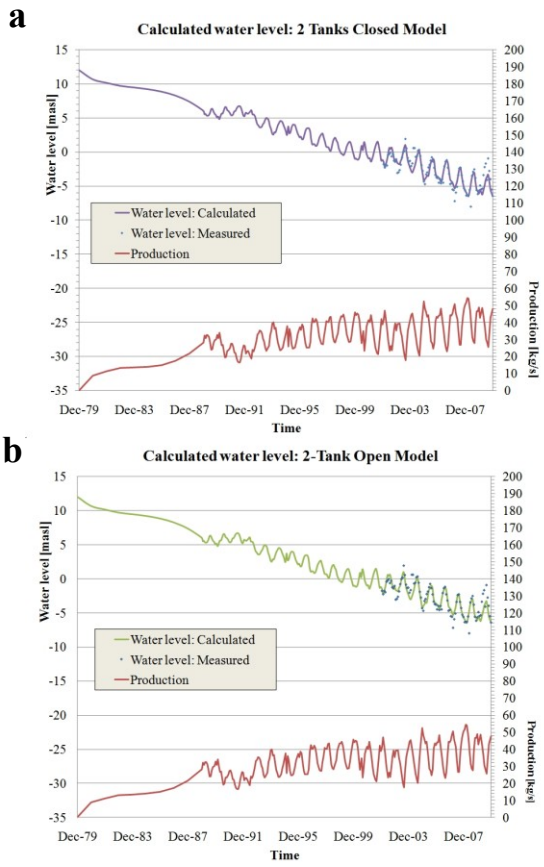

Figure 13: Simulation results of the lumped-parameter modeling process. a) 2-tanks closed, b) 2-tanks open.

Table 3: Summary of statistical parameters and coefficients of storativity and mass conductance evaluated by LUMPFIT.

Model number	1	2	3	4
Number of tanks	1	1	2	2
Model type	Closed	Open	Closed	Open
κ (m s²)				
κ1	156246	4364.76	1173.41	1166.84
κ2			242395	234923
σ (m s)				
σ1		2.69E-4	7.54E-4	7.57E-4
σ2				2.07E-5
R^2 (%)	53.350	60.998	82.993	**83.005**
RMS misfit	1.440	1.317	0.869	0.869
Std. dev.	1.448	1.332	0.885	0.889

The coefficient of storage (κ) can be used to evaluate the size of the reservoir. The storage in a liquid-dominated geothermal system, like the OBGA, can result from two different kinds of storage mechanisms (Axelsson, 1989). In the first case, this parameter is controlled by liquid/formation compressibility. The following relation ensues:

$$\kappa = V\rho[\varphi c_w + (1-\varphi)c_r] \quad (8)$$

Where V represents reservoir volume, ρ is the liquid density, φ is the porosity, c_w is the compressibility of water (i.e. 5.0E-10 Pa^{-1}) and c_r is the compressibility of the rock matrix (i.e. 2.0E-11 Pa^{-1}). Alternatively, storage can be controlled by the mobility of a free surface. In that case, the storage coefficient is given by the relation:

$$\kappa = \frac{A\varphi}{g} \quad (9)$$

Where A is the surface area of the modeled portion of the reservoir and g is the acceleration of gravity. The storage coefficients for the 2-tank models were substituted in equations (8) and (9). The volume and surface area parameters can be calculated. The results are presented in Table 4.

Table 4: Comparison between reservoir size estimations from lumped parameter and volumetric modeling.

Storage Mechanism	No. of Tanks	2	2	Volumetric Model	
	Model Type	Closed	Open	Cons.	Opt.
Compressibility	Volume (km^3)	*4200*	*3683*	11.8	30.2
Free-surface mobility	Surface Area (km^2)	**23.9**	**23.1**	16.4	45.4

Because of spatial constraints, the volume values calculated for the case of compressibility-dominated storage are unacceptable. For the case of free surface mobility, the surface area obtained from the 2-tank open model (i.e. 23.1 km^2) is comparable to the areal interval defined for the volumetric model (i.e. 16.4-45.4 km^2).

From these results it can be concluded that the OBGA is an open system whose storage is controlled by the mobility of a free surface (i.e. unconfined reservoir). Furthermore, it seems both volumetric and lumped parameter modeling agree with a reservoir extent contained somewhere within the boundaries defined in Figs. 9-10.

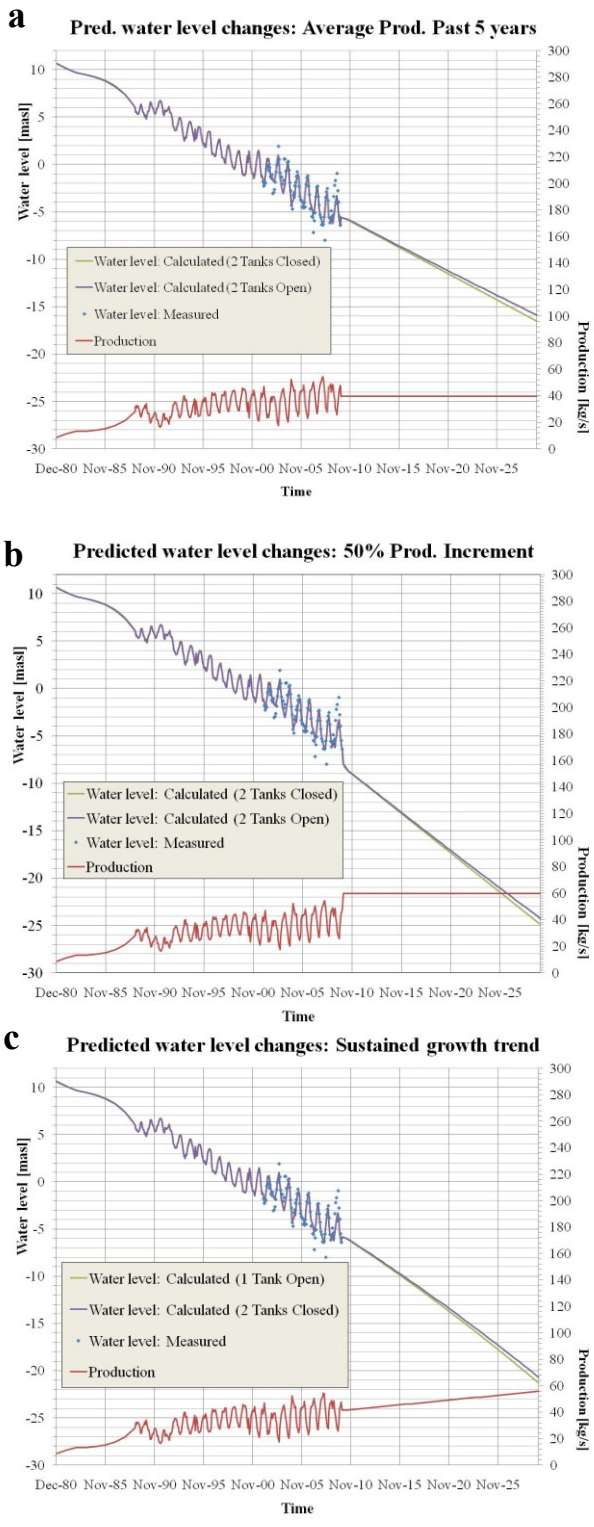

Figure 14: Projected response for the next 20 years. Different production scenarios considered a) 40 kg/s, b) 60 kg/s, c) sustained growth trend.

Another application of lumped-parameter models is the evaluation of the future response of the reservoir. Three production scenarios are defined for the next 20 years. The first scenario maintains the average production rate observed over the last 20 years (i.e. 40 kg/s). The second scenario considers an increment of 50% on the same rate (i.e. 60 kg/s). The third scenario assumes the growth in production rate observed over the past 20 years is sustained for the next 20 years. Figure 14 contains the results of these simulations.

The differences between optimistic and conservative estimates in the three scenarios are relatively small. The water level decreases in the first scenario at a rate of 47-50 cm/a. In the second scenario, water level drops at a rate of 89-92 cm/a. In the third scenario, the projected water level drop occurs at a rate of 71-74 cm/a. These rates can be extrapolated in the long run. After 100 years, the water level is expected to be 47-92 m lower. Similarly, the water level is projected to drop 140-275 m in 300 years. These cases are manageable by readjustment of the pumping equipment at the wells. The effects of reinjection were outside the scope of this paper.

CONCLUSION

The Olfus-Bakki Geothermal Area is an open system where volcanic chlorinated fluids from the Hveragerdi high-temperature geothermal field migrate to the south following the hydraulic gradient. Meteoric water enters the reservoir by infiltration through the surface faults, mixing with the volcanic waters. One location of recharge was identified in the Ingolfsfjall zone. The unmixed volcanic water keeps its southbound migration. The Nupar lineament restricts groundwater flow and creates a divergence in the flow path. The fluids to the left of this barrier are confined in the Thoroddstadir zone (well ÞS-01) by the Bakki lineament. Another recharge zone was identified in this region, where mixing with meteoric water is suspected. The fluids to the right of the Nupar lineament reach the Bakki field, converging in this point with fluids from Hlidardalskoli (well HS-02) and with fluids of marine origin. It is suspected that small lenses with old water of glacial origin are dispersed throughout the OBGA. Figure 15 summarizes these processes.

ACKNOWLEDGEMENTS

This paper was possible thanks to the data and financial support provided by Reykjavik Energy and by the data provided by ÍSOR.

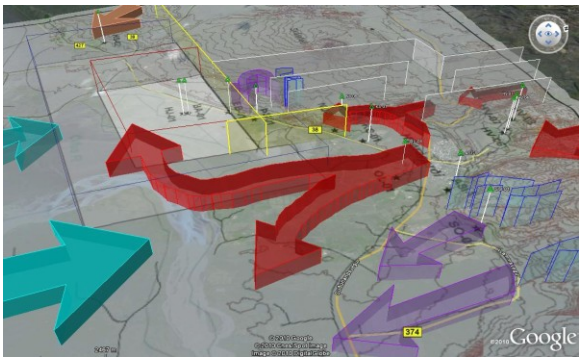

Figure 15: Schematic visualization of the OBGA. Volcanic waters are represented in red, mixed waters in purple and marine waters in cyan. The Bakki and Nupar lineaments are represented as yellow walls. Surface faults where recharge occurs are seen in blue. The Bakki field is delimited by red and blue lines (as showin in Fig. 9). Added content to image from Google™.

REFERENCES

Aradóttir, A. (2010a). *Water production for the Thorlakshofn district heating system 2009* (In Icelandic). Reykjavik Energy Internal Report. pp. 1-21. Reykjavik.

Aradóttir, A. (2010b). *Water production in the Olfus region (In Icelandic)*. Reykjavik Energy Internal Report. pp. 1-18. Reykjavik

Arnórsson, S., & Andrésdóttir, A. (1995). *Process controlling the distribution of boron and chlorine in natural waters in Iceland*. Geochimica et Cosmochimica Acta. **59** (20), 4125-4146.

Arnórsson, S., Andrésdóttir, A., Gunnarsson, I., & Stefánsson, A. (1998). *New calibration for the quartz and Na/K geothermometers--valid in the range 0-350 °C*. (In Icelandic). Proc. Geoscience Society of Iceland Annual Meeting, (pp. 42-43). Reykjavik.

Axelsson, G. (1989). *Simulation of Pressure Response Data From Geothermal Reservoirs By Lumped Parameters*. XIV Workshop on Geothermal Reservoir Engineering. pp. 1-7. Stanford, CA: Stanford University.

Axelsson, G., & Arason, P. (1992). *Lumpfit User's Guide, version 3.1*. pp. 1-32. Reykjavik: Orkustofnun.

Axelsson, G., Bjornsson, G., & Quijano, J. (2005). *Reliability of Lumped Parameter Modeling of Pressure Changes in Geothermal Reservoirs*. pp.

1-8. Proceedings World Geothermal Congress. Antalya, Turkey.

Giggenbach, W. (1991). *Chemical techniques in geothermal exploration*. In F. D'Amore, Application of geochemistry in geothermal reservoir development. pp. 119-142. Rome: UNITAR/UNDP publication.

Giggenbach, W. (1988). *Geothermal solute equilibria. Derivation of Na-K-Mg-Ca geoindicators*. Geochim. Cosmochim. Acta. **52**, 2749-2765.

Gonzalez-Garcia, J. (2011). *Reservoir assessment of the Ölfus-Bakki low-temperature geothermal area, SW Iceland*. MSc thesis. Reyykjavik: University of Iceland.

Stefánsson, V., & Steingrímsson, B. (1990). *Geothermal Logging I: An introduction to techniques and interpretation*. pp. 1-110. OS-80017/JHD-09. Reykjavik: Orkustofnun.

.